



Fellenius, B.H., 2013. Capacity and load-movement of a CFA pile: A prediction event. ASCE GeoInstitute Geo Congress San Diego, March 3-6, 2013, Foundation Engineering in the Face of Uncertainty, ASCE, Reston, VA, James L. Withiam, Kwok-Kwang Phoon, and Mohamad H. Hussein, eds., Geotechnical Special Publication, GSP 229, pp. 707-719.

## Capacity and Load-Movement of a CFA Pile. A Prediction Event

Bengt H. Fellenius<sup>1</sup>, P.Eng., M.ASCE

<sup>1</sup>Consulting Engineer, 2474 Rothesay Avenue, Sidney, BC, V8L 2B9; bengt@fellenius.net

**ABSTRACT** A static loading test on a 406 mm diameter, strain-gage instrumented, 18.5 m long CFA pile presented an opportunity for arranging an impromptu prediction event. Several people known to be interested in deep foundation challenges were invited to submit a prediction of capacity and load-movement response of the pile ahead of the testing. Despite that the window of time was a mere week, no fewer than 41 persons responded, representing 15 countries and most continents. The soil profile at the site consisted of a transported and redeposited silty sandy medium plastic, very stiff, ablation clay till containing lenses of sand and gravel categorized by SPT N indices and a few water contents. Concern for safety of the test arrangement forced the static loading test to be aborted when the applied load was 1,790 KN before any tendency toward an ultimate resistance had developed. However, the extrapolated load-movement curve was used as reference to the predicted load-movement curves. Strain-gage instrumentation indicated a low E-modulus commensurate with the mere 13-day wait time between constructing and testing the pile. The records also indicated that only about 500 of the maximum applied load had reached the pile toe when the test was aborted. The paper presents the results of the test, the approach to determining the pile modulus from the strain-gage data, the load distribution, and extrapolated pile-head load-movement curves for reference to the predicted curves. The predicted values of pile capacity ranged from a low of 830 KN through a high of 3,600 KN with an average of 1,920 KN. Thirty-six of the predictions included the pile head movement at the predicted capacity and the movements ranged from 8 mm through 220 mm with an average of 35 mm. Clearly, the predictors' definitions of pile capacity differed. The compilation of the predictions presented in the following include bell curve distributions of submitted capacities and movements, showing that the widths of two standard deviations, thus encompassing two-thirds of all values, for capacity and movement were 1,090 KN and 2,760 KN and 9 mm through 61 mm, respectively.

### INTRODUCTION

Occasionally, so-called prediction events are arranged, wherein geengineers in various fields of specialization are asked to predict the outcome of a full-scale pile test. The participants are presented with information on the soil conditions at a specific site, details on a pile to be subjected to the test, and the testing programme. Some of the events can be very ambitious, e.g., the ASCE Evanston event (Finno et al. 1989a; 1989b) or more casual, e.g., the ASCE and PDCA Orlando, Florida event (Fellenius et al. 2004).

A prediction event is often organized as a part of a conference and it can be a very entertaining. It is often believed that (1) the analyses presented are representative for the state-of-the-art, and (2) that the individual, "the Winner", who entered a prediction that is the closest to the test results is most competent in the field of designing piled foundations. However, this is only marginally true. The state-of-the art of designing piles and piled foundations requires assessment of much more information than typically is provided in a prediction event. The predictions do, however, offer a snapshot of the approach to the analysis as practiced in different countries, states, geologies, industries, etc., as well by different authorities, codes, and standards.

As to the “Winner”, the actual test results lie usually somewhere within the range of responses and somebody within that range is bound to be close to the actual. Regardless of how close or not to the actual test results a prediction is, its value lies in its presentation of the reasoning and justification behind the particular analysis method used to develop the prediction, particularly so when it is compared to those of the other participants. Nevertheless, there is a definite personal satisfaction, indeed pride, in getting it close. There is also its opposite, and many have shown a reluctance in taking on the challenge and face the risk of getting it “wrong”, preferring instead to comment on the relative merit of the predictions after the event; indeed, at times offering a superior “prediction”. It is surprising that so many are reluctant to put their name under a prediction, but have no qualms writing a geotechnical report to a client with recommendations for a design. A possible explanation lies in that when one is wrong in a geotechnical report—by definition, also a prediction—one can hide behind an insurance policy, whereas getting egg on one’s face in a public event is very visible, and there is no place to hide.

In May 2011, when a static loading test was to be performed on a 406 mm diameter, 18.5 m long CFA test pile constructed at a previously untouched industrial site north of Edmonton, Alberta, I saw this as an opportunity for a prediction event. I contacted a good number of persons known to be experienced in the response of piles to load and, although the window they were given for delivering a prediction was only about a week, no fewer than 41 individuals, representing 15 countries and most continents, responded with a prediction of capacity, and 35 of these also predicted the load-movement for the test pile. This paper presents the results of the static test, a compilation of the predictions received, and discusses the range of capacities predicted as well as the uncertainties and the rather large range of movements assigned to the capacities.

## SOIL PROFILE

According to Kathol & McPherson (1975), the bedrock in the general area of Edmonton, Alberta, was created in Cretaceous times and consists of bentonitic shale and sandstone with coal seams. The elevation of the bedrock surface varies, while the ground surface is generally level, which means that the thickness of the overburden varies. Three Quaternary soil types dominate the soil profile. From the ground surface, the soil layers consist of (1) layers of lacustrine sand, silt, and clay with alluvium inclusions of sand and silt and, occasionally, aeolian sand, (2) glaciolacustrine sand, silt, and clay, and (3) glaciofluvial sand and gravel. The origin of these layers is glacial tills in the Rocky Mountains, which soils were water-transported to the area and deposited in glacial lakes on existing ablation till. Between the till and the bedrock, the soils consist of Tertiary gravel and sands containing coal fragments and clay lumps. The groundwater table lies close to or a few metre below the ground surface and the pore pressure distribution is usually hydrostatic. In many places, aquifers exist in buried valleys and exhibit non-hydrostatic pressure with regard to the groundwater table.

Soil borings at the specific site showed the soil profile to consist of a glacio-lacustrine clay and silt to about 10 m depth with a water content ranging from about 30% through about 40% with plastic and liquid limits of about 25% and 60%. The SPT N-indices indicated soil conditions to be soft ( $N \leq 4$  bl/0.3m) above about 7 m and stiff to very stiff ( $8 \leq N \leq 15$  bl/0.3m) below 7 m depth. From about 10 m depth to 25 m depth (the deepest borehole was 25.6 m), the soil consisted of very stiff ( $15 \leq N \leq 30$  bl/0.3m) ablation clay till with lenses of sand and, silt, and a water content ranging from about 15% through about 20%. The groundwater table was about 1.5 m below grade and the pore pressure distribution was assumed to be hydrostatic.

Figure 1 shows the distributions of natural water content and SPT N-indices from two boreholes close the test pile location. No cone penetrometer sounding (CPTu) was included in the testing programme, and no deep piezometer was installed. No laboratory testing beyond determining water content was performed.

**TEST PILE**

The test pile was a nominal 406 mm diameter continuous flight auger (CFA) pile drilled to a depth of 18.5 m on April 25, 2011. The lowest 1.0 m length was tapered. The pile was concreted the day after. Continuous monitoring of the construction with regard to profile, concrete volume, drill rate, torque, and rotation of auger showed a 30% overconsumption of concrete, but no signs of necking or bulging. Immediately after concreting, a 200 mm diameter reinforcing cage was pushed into the concrete to a depth of 17.0 m. The cage consisted of five 20 mm reinforcing bars and a 9 mm diameter spiral reinforcement on 230 mm spacing (rise). One pair of Geokon vibrating wire strain gages were attached to the reinforcing cage at depths of 16.2 m (GL1), 12.2 m (GL2), 8.1 m (GL3), and 1.6 m (GL4). The gages were read before placing the cage in the pile, when the cage had been placed, and every minute during the wait time until the start of the static loading test. No telltales were placed in the pile. Figure 1 includes a sketch showing the pile depth and the depths of the strain gage pairs. Figure 2 shows the arrangement at the pile head.

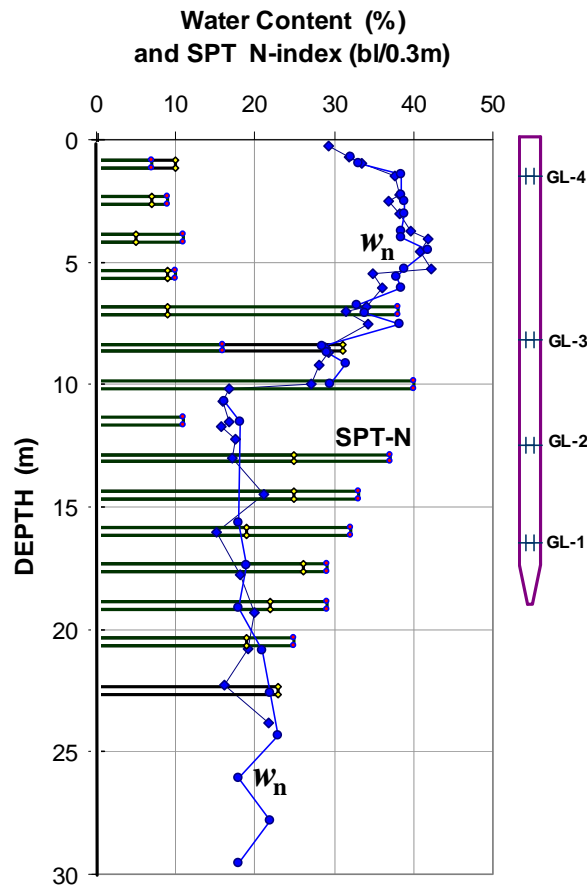


Figure 1. Distributions of water content and SPT-N indices

After completion of the test pile, four anchor piles were installed around the test pile to depths of 18.0 m. The distance between the test pile and the anchor piles was 4.0 m. Each anchor pile was connected via a Dywidag bar to a system of beams transferring the load from the jack on the pile head to the anchor piles. A displacement gage was attached to two anchor piles to monitor upward movement.

## TEST SCHEDULE

The pile load was applied by a jack operated by an automatic load-holding pump. The pile head movement was monitored with four linear voltage displacement transducers (LVDT) connected to a data logger. The load applied to the pile was measured with a load cell also connected to the data logger. As a back-up and alternative system, the jack pressure and the pile head movement were recorded by taking manual readings of the jack manometer and two separate dial gages. The test method was the quick maintained-load method per the ASTM D1143 Guidelines. The test schedule was to load the pile in increments of 150 kN until failure. Increments were applied every 10 minutes and the load levels were held constant between adding increments.



Figure 2. Arrangement at the pile head

The static loading test commenced on May 9, 2011, on the 13th day after the concreting of the test pile. After the first couple of increments had been applied, it became clear from reference to the jack pressure that the load cell calibration factor was incorrect and the magnitude of the actual load increment was about 100 kN, which was smaller than the intended 150-kN value. However, rather than determining the correct calibration factor (which would have required unloading the pile), it was decided to stay with the increment magnitude value and determine the actual magnitudes of load after the test.

When the applied load had reached about 1,600 kN, it was noticed that one anchor pile was moving progressively upward, and sharp sounds indicated that the reaction system was adjusting to differential movements of the beam supports. Therefore, it became obvious that further increase of load was not advisable, and the pile was unloaded and the test terminated. The maximum applied load was 1,795 kN.

## RESULTS

### Observations Before the Start of the Static Loading Test

The temperature and strains measured before the start are shown in Figure 3. The values are referenced to the “zero” reading taken immediately before lowering the cage into the pile. The soil temperature near the ground surface (GL4) was affected by the low temperature of the winter just past, whereas the soil deeper down in the ground was warmer, about 8°C, which is equal to the annual mean temperature in the area. During the first about 12 hours, the concrete, which was delivered with a temperature of about 20°C, was cooled by the soil, but, when the hydration process started, the cooling rate first slowed down and, then, the temperature increased, reaching a peak after a further about 40 hours after the insertion of the cage. The concrete then cooled again, and at the time of the test start, the temperature was close that of the soil at the gage depths.

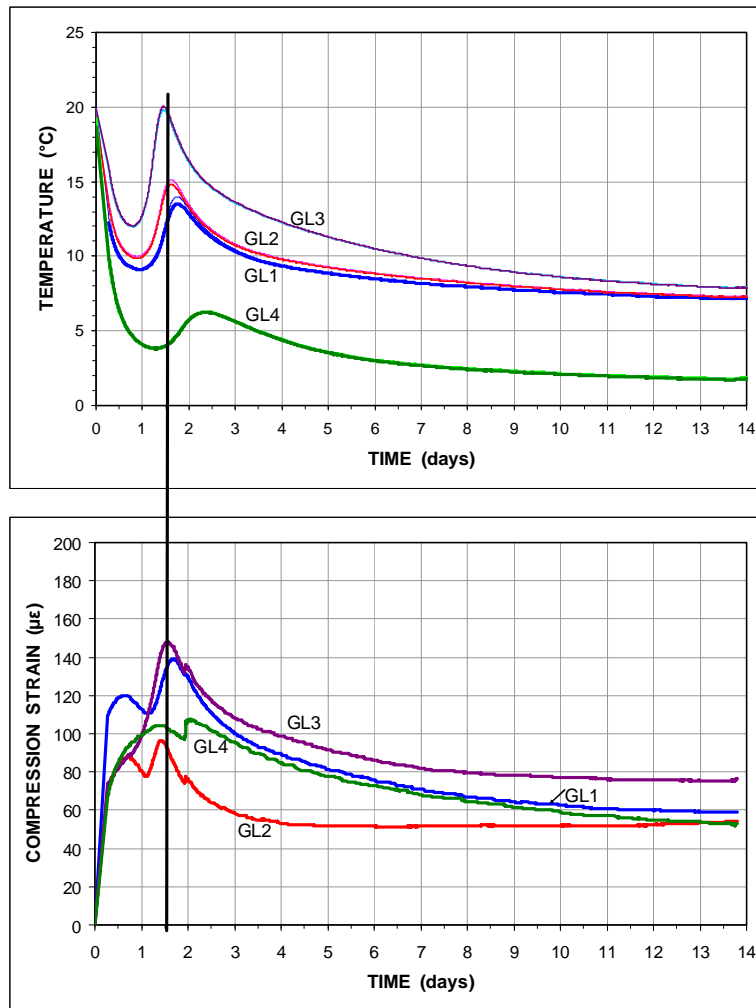


Figure 3. Temperature and strain during the wait time before the start of the static loading test

The strain measurements showed that the axial compression increased by about 100  $\mu\epsilon$  at all gage levels during the first few hours. When the hydration process started, at GL1 and GL2, a reduction in strain was observed, but no such reduction was measured at GL3 and GL4. The development of temperature and strain were qualitatively similar to those measured by Fellenius

et al. (2009), only smaller in magnitude. The compression strain increase is for the most part not an effect of shear forces developing along the pile, but by the fact that the thermal expansion of the hardening concrete is smaller than that of the steel in the gages. Therefore, compression strain was introduced in the gages by the fact that the thermal expansion of the steel gage was restrained by the concrete, resulting in an apparent compression. (The difference of strain readings due the actual difference in thermal coefficient is corrected for). The compression in the gage corresponds to a similar tension in the concrete, and there is little or no correlation to shear between the pile and the soil. Possibly, during the about two weeks wait period, some compression strain could also be due to residual load developing in the pile, as discussed later on in this paper.

### Results of the Static Loading Test

Figure 4 shows the measured pile-head load-movement curve. The maximum load applied was 1,795 KN, and the pile head movement at this load was 11 mm. At this load, the pile capacity was not mobilized. Figure 5 shows the measurements of the individual strain gages at the four gage levels GL1 through GL4 during the static loading test and 40 minutes after the unloading of the pile. The measurements showed all gages to function well.



Figure 4. Pile-head load-movement curve

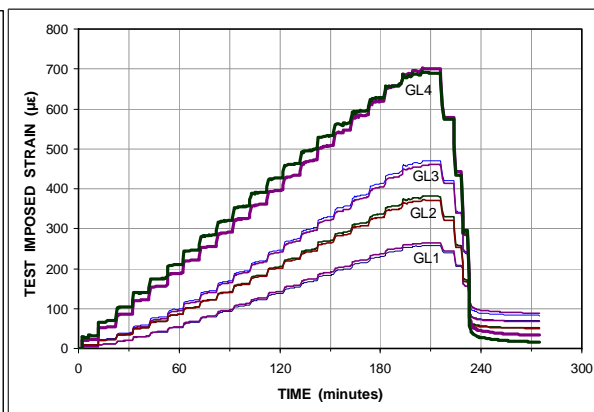


Figure 5. Strains measured during loading and unloading, and 40 minutes after unloading

Before measured strains can be converted to axial load in a pile, the pile modulus correlating strain to load must be known. The modulus of concrete is a function of cement amount, mineral type and properties, and other aspects. Its correlation to cylinder strength is very poor. It is also not a constant, but diminishes with increasing stress. However, provided that the range of strain imposed in the test is large enough, in excess of at least  $400 \mu\epsilon$ , then, the modulus can be determined directly from the applied values of load and measured strain as indicated by Fellenius (2001; 2012).

The correlation between stress and strain, the stiffness,  $AE$ , is best determined by analysis of the records from a gage level close to the pile head, where there is no influence from shaft resistance. The load-strain relation for a concrete pile is not linear, but a secant stiffness,  $AE_s$ , defined as load/strain,  $Q/\epsilon$ , can be assumed to be reasonably linear function of strain,  $\epsilon$ . The load for a certain value of strain is then simply the secant stiffness times the strain value. The problem with the  $AE_s$  line, when determined directly by  $Q/\epsilon$ , i.e., by the secant stiffness method, however, is that it depends very much on the validity of the starting value of strain. An initial error of strain will be present in all values of strain and even a small value can result in significant error in the evaluated stiffness (Fellenius 2011).

A second limitation of the direct evaluation of the secant stiffness approach lies in that it can only be applied to the strain-gage values obtained in the gage level nearest the pile head, and, then, only if that gage level is so close to the pile head that it is unaffected by shaft resistance. Both limitations are avoided by instead using the tangent stiffness method, also termed the incremental stiffness method. The tangent stiffness method plots the ratio of the change of load to change of strain,  $\Delta Q/\Delta \epsilon$ , or  $(Q_n - Q_{n-1})/(\epsilon_n - \epsilon_{n-1})$ , versus strain,  $\epsilon$ . Once the shaft resistance is fully mobilized along the portion of the pile between the gage level and the jack, the tangent stiffness line,  $AE_t$ , will develop. The slope of the line is equal to  $AE_{start} + k\epsilon$ , where “k” the slope (always negative). The secant stiffness is then simply a line starting from the same stiffness,  $AE_{start}$ , but having half the slope, i.e.,  $0.5 k$ .

The tangent stiffness method is a differential method, however, and the results depend very much on the ratio between the accuracy, i.e. the imprecision or error, in the applied load to the accuracy of the increment. If the imprecision ratio is too large, the resulting values will not plot along a well defined line, but be rather scattered.

The two methods for determining the pile stiffness,  $AE$ , were applied to the test data. Figure 6 shows the results of the secant method applied to the GL4 strain records. Figure 7 shows the incremental (tangent) stiffness versus increasing strain for the four gage levels. As shown, the secant relations determined by secant stiffness and the tangent stiffness methods were equal, which indicates that the GL4 data did not include extraneous strains values. The records from every load level (every increment) showed a bit of scatter, which was a result of the small load increments. To filter the results, the sliding alternative selection was chosen, where every second line, i.e.,  $(Q_n - Q_{n+2})/(\epsilon_n - \epsilon_{n+2})$ , was used, still stepping the analysis one line at a time. This removed most of the scatter.

Figure 7 also shows that at the maximum applied test load, the incremental stiffness values from GL3 were just about to approach the tangent stiffness line, but had not yet done so, when the test was aborted. That is, even for the maximum load applied, the shaft resistance immediately above and below GL3 was not fully mobilized.

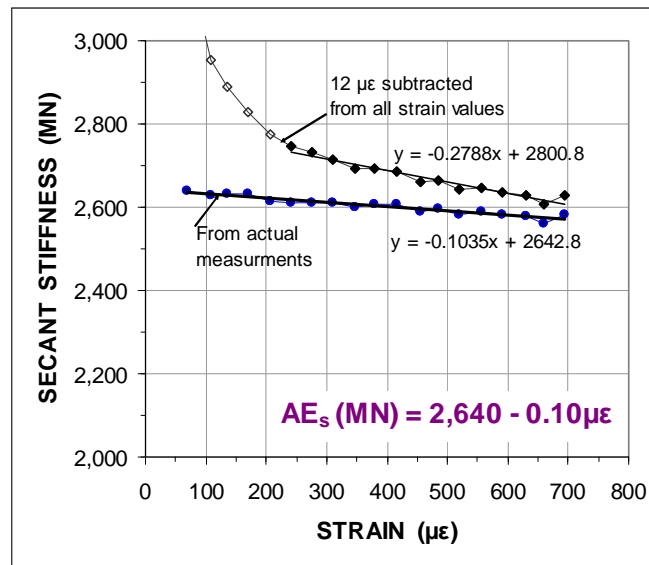


Figure 6. Secant stiffness versus strain from GL4

The axial secant stiffness of the pile follows relation  $AE_s = 2,640 - 0.10\mu\epsilon$ , that is, the reduction with increasing strain is minimal. This relation converts the strain of  $695 \mu\epsilon$  measured at GL4 nearest the pile head at the maximum load of 1,795 KN applied to the piles head to a load of 1,786 KN, which is practically equal to the maximum test load. The load distribution evaluated

from the strain records for the secant stiffness relation are shown in Figure 8. The shaft resistance distribution curve connecting the gage level loads was extended to the pile toe, which indicated a mobilized toe resistance of 500 KN. No measurements of pile toe movement were taken. However, the average strain imposed in the pile at the maximum test load was 350 to 400  $\mu\epsilon$ , which corresponds to a pile shortening of about 8 mm. At the maximum load, 1,795 KN, the pile head movement of 11 mm, the pile toe movement might have been about 2 to 3 mm.

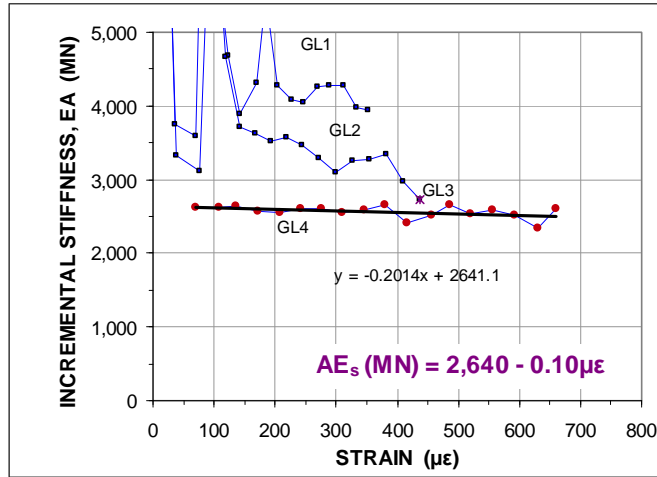


Figure 7. Tangent stiffness versus strain from all gage levels filtered by second line selection

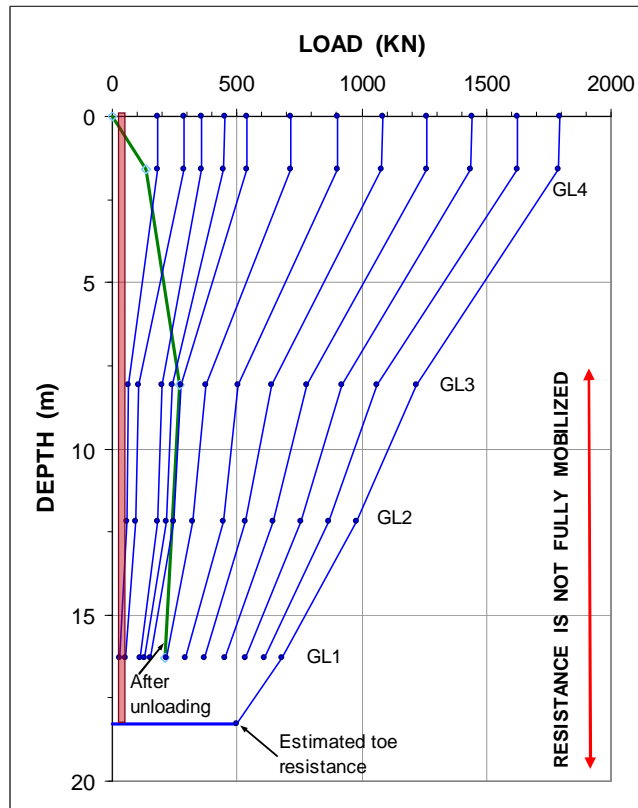


Figure 8. Load distributions

Between the pile head and GL3 at 8.1 m depth, the shaft resistance amounted to 565 KN. An effective stress analysis for the upper 8.1 m shows that this amount of shaft resistance—just about mobilized—corresponds to a beta-coefficient of 1.0. (The analysis takes into account that the 30% overconsumption of concrete corresponds to 15% increase in shaft diameter and shaft circumference). Usually, however, the shaft resistance in the upper glacio-lacustrine clay and silt corresponds to a beta-coefficient of about 0.4 to 0.5. It is likely that the test pile is subjected to a fully developed residual load in the clay and silt above GL3. If corrected for residual load, fully mobilized shaft resistance in the till below 10 m depth would be expected to correspond to a beta-coefficient of ranging from about 0.8 through 1.0.

While the prematurely terminated loading still provided results that were useful for the design of the piled foundations of the intended building, the results were of limited use for the prediction event. To improve its value as reference to the predictions, the load-movement curve was extrapolated. Three separate extrapolations were made.

First, a hyperbolic function was fitted to the measured pile-head load-movement curve and the fitted curve was extrapolated to 30 mm total pile head movement. Second, the pile load response was calculated in an effective stress analysis employing the UniPile program (Goudreault & Fellenius 1999) with input of the soil profile and a beta-coefficient of 0.5 above the depth of GL3 and 0.9 below. It was assumed that residual load was fully mobilized in the upper 10 m and tapered off linearly from that depth to the pile toe, i.e., no residual toe load. The shear-movement response along the pile shaft, was modeled by two alternative t-z functions. One was the “ratio function”, i.e., the ratio between any two loads is equal to the ratio between their movement values raised to an exponent. The exponent used was 0.2, and it was assumed that the beta-coefficient represented the shear force developed at a relative movement of 5 mm. The second t-z function was a custom function that reached a value equal to the shaft resistance determined by the beta-coefficient at a movement of 5 mm, increasing to 110% load at 15 mm movement, whereafter it softened back to 100% at 50 mm movement. It was further assumed that also the pile toe load-movement followed a ratio function, now with an exponent of 0.5 and that the 500 KN toe resistance developed at a movement of 3 mm. The pile E-modulus was taken from the 2,600 MN stiffness value.

Figure 9 shows the test curve (unloading and unloading) and the three fitted and extrapolated curves using t-z and q-z functions for the soil response. While I feel that the curves fairly represent the upper and lower boundaries of the test pile load-movement response, an actual test might well have shown results outside the boundaries.

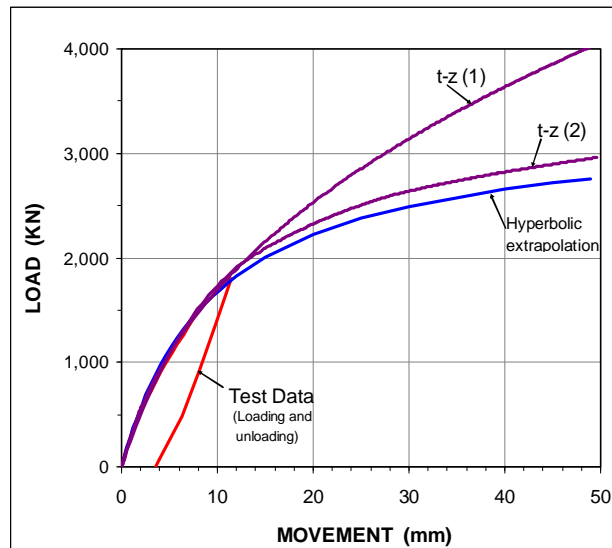


Figure 9. Measured and extrapolated load-movement curves

## PREDICTIONS

A total of 41 predictions were received and 35 of those included full pile-head load-movement curves. The predictions are compiled in Figure 10. The six capacity values that were not accompanied with load-movement data are plotted at 50 mm movement. The figure also includes the load-movement of the test and the boundary curves shown in Figure 9.

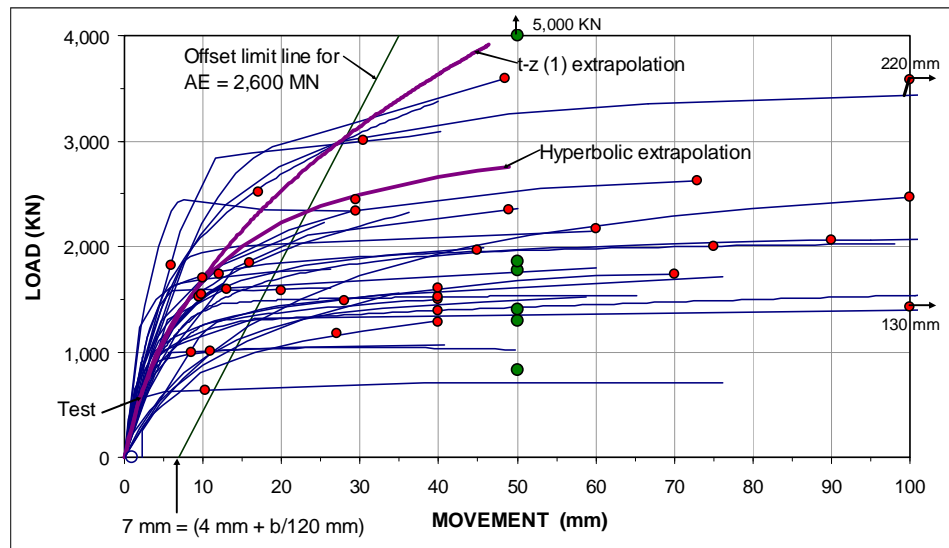


Figure 10. Predicted capacities and pile-head load-movement curves with curves extrapolated from the test

Disregarding the smallest and largest values, the predicted values of pile capacities ranged from a low of 830 KN through a high of 3,600 KN with an average of 1,920 KN. The bulk of values were within about 1,000 through 3,000 KN. Most predictors appear to have chosen the capacity value from some judgment of the shape of the load-movement curve. A couple indicated that the offset-limit method had been used to determine the capacity value. Four gave as capacity the load that resulted in a pile head movement of 10% applying the common misconception of that this is the definition once recommended by Terzaghi (Likins et al. 2011).

It is not surprising that the predicted capacities showed a large scatter. No predictors were familiar with the type of soil at the site; besides, nobody knew where the site was located. Indeed, the scatter of results does not mean that the predictors were not able to estimate the response of a pile to load, but it does emphasize that knowledge from previous pile response in the geology of the test site is essential. Coincidentally, the mean of the predicted capacities was about equal to the test load applied when the test was aborted. Figure 11, shows a bell-curve distribution of the predicted capacities, emphasizing the scatter. Figure 12 shows a bell-curve of the predicted movement for those capacities.

The variation of movement at the capacity is further emphasized in Figure 13 showing all the predicted load-movement curves normalized by setting each capacity equal to 100 and all loads adjusted in proportion, but keeping the movement values intact. The large scatter of movement values is much more of a surprise than the scatter of capacity values. At a value of half the capacity, i.e., at a factor of safety of 2.0, the predicted movements range from 2 mm through 35 mm. That so many of the predictors would base their capacity values on very large movement deserves attention. Most codes and standards only deal with “capacity”; moreover, they rarely define what would constitute a “capacity” of a pile. This is an unsafe situation that merits attention from the practitioners.

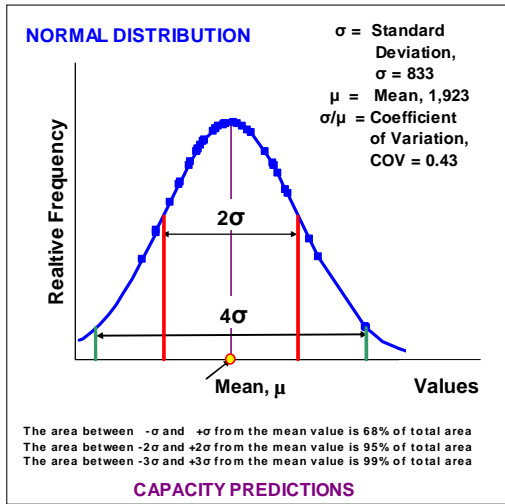


Figure 11. Normal distribution of the predicted capacities

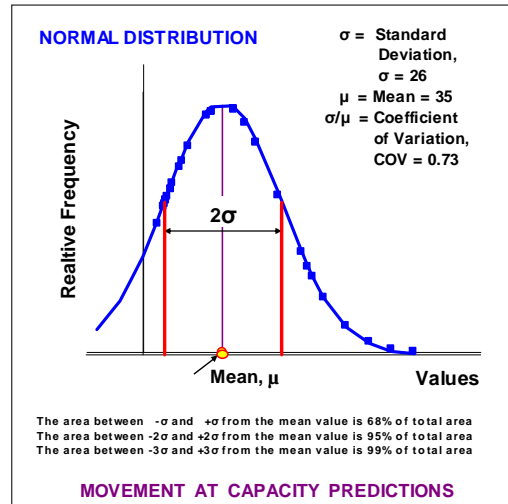


Figure 12. Normal distribution of the predicted movements

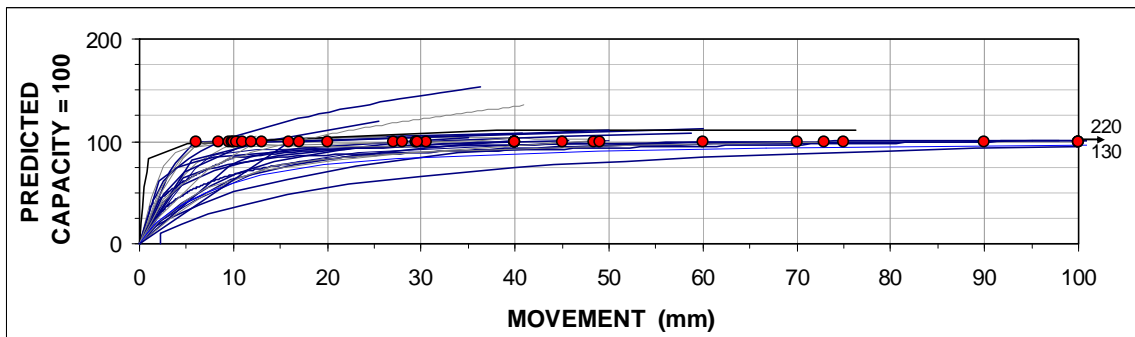


Figure 13. Normalized predicted capacities versus predicted load-movements

Indeed, codes appear to be based on the belief that applying a factor of safety or a resistance factor to a capacity will result in a safe working load or an acceptable factored resistance and a sound foundation with no more than acceptable settlement. This is far from always correct. The reverse, a piled foundation shown in a reliable settlement analysis to be within settlement tolerances will generally also show to have acceptable magnitude of load from a capacity aspect.

**CONCLUSIONS**

Although the static loading test had to be prematurely interrupted, the imposed strains were large enough to enable determining the pile modulus and the load distribution for the test. The evaluated effective stress parameters (beta-coefficients) were within those expected for the soil conditions. However, the fact that the test did not move the pile sufficiently so as to fully mobilize the shaft resistance along the pile makes the results of detailed analysis mostly speculative.

The measured pile-head load-movement curve was fitted using input of t-z functions and the approximately established beta-coefficients. The load-movement was then extrapolated beyond the measured maximum movement to establish an estimated set of pile-head load-movement curves within reasonable boundaries for use to compare to the predicted load-movement curves.

The predicted capacities varied within a large range. For the bulk of the predictions, the largest capacity was three times the smallest. Had the predictors been knowledgeable of the site and previous actual response of piles to load, most likely the scatter would have been much smaller. The scatter mainly emphasizes the need for experience of a local geology in making design calculations.

That the movements at the predicted capacity values would be so widely ranged and disparate is a surprise, however. That several of the capacities interpreted from the predicted load-movement curves were chosen at very large movements imply a current inconsistency and uncertainty in the profession that gives concern for the validity of blanket application of safety or resistance factors to capacity values.

## ACKNOWLEDGMENTS

The piles were installed by North-American Construction Group, Edmonton, Alberta. The test pile was instrumented and the test was run by AATech Scientific Inc. Ottawa, Ontario. The author is indebted to Mr. Hicham (Sam) Salem, M.A.Sc., P.Eng., AATech Scientific Inc. for use of the data and for the many enlightening discussions with regard to this test and others.

## PREDICTORS

The following person submitted a prediction for the test. For a couple of the listed persons, the prediction was a joint effort.

|                     |             |                    |         |
|---------------------|-------------|--------------------|---------|
| Stephen Buttlng     | Australia   | John Hayes         | USA     |
| Harry Poulos        | Australia   | Nicole Lavergne    | USA     |
| Peter Van Impe      | Belgium     | John Livingston    | USA     |
| Luciano Decourt     | Brazil      | Paul Mayne         | USA     |
| Lech Brzezinski     | Canada      | Ross McGillivray   | USA     |
| Bengt H. Fellenius  | Canada      | James Niehoff      | USA     |
| Munawar Hussain     | Canada      | Mauricio Ochoa     | USA     |
| Mats Mets           | Estonia     | Kathryn Petek      | USA     |
| Kazem Fakharian     | Iran        | Ha Pham            | USA     |
| Joram Amir          | Israel      | Frank Rausche      | USA     |
| Phan Le             | Japan       | Greg Reuter        | USA     |
| Tatsunori Matsumoto | Japan       | Tim Siegel         | USA     |
| Manuel J. Mendoza   | Mexico      | Jim Stewart        | USA     |
| Jaime Santos        | Portugal    | Mark Thompson      | USA     |
| Sun Jie             | Singapore   | Luu Van Dong       | Vietnam |
| Harry Tan           | Singapore   | Nguen Xuan Hai     | Vietnam |
| Hartano Wu          | Singapore   | Nguyen Minh Hai    | Vietnam |
| Gianni Togliani     | Switzerland | Nguyen Truong Tien | Vietnam |
| Ha Da               | USA         | Quan Duy Nguen     | Vietnam |
| Tom Gurtowski       | USA         | Trinh Viet Cuong   | Vietnam |
| Fouad Hammoud       | USA         | Vu Cong Ngu        | Vietnam |
| Dean Harris         | USA         |                    |         |

**REFERENCES**

- Fellenius, B.H. (1986). *The FHWA static testing of a single pile and a pile group—Report on the analysis of soil and installation data plus Addendum Report*. FHWA, Washington, Prediction Symposium, 13p.
- Fellenius, B.H. (2001). From strain measurements to load in an instrumented pile. *Geot. News Mag.*, 19(1) 35-38.
- Fellenius, B.H. (2012). Critical assessment of pile modulus determination methods. Discussion. *Can. Geo. J.*, 49(5) 614-621.
- Fellenius, B.H. (2012). *Basics of foundation design*, a text book. Revised Electronic Edition, [www.Fellenius.net], 384p.
- Fellenius, B.H., Hussein, M., Mayne, P. and McGillivray, R.T. (2004). Murphy's Law and the pile prediction event at the 2002 ASCE Geo-Institute's Deep Foundations Conference. *Deep Found. Inst. Current Practice and Future Trends in Deep Foundations*, Vancouver, September 29-October 1, pp. 29-43.
- Fellenius, B.H., Kim, S.R. and Chung, S.G. (2009). Long-term monitoring of strain in instrumented piles. *J. Geo. and Geoenv. Engng.*, 135(11) ASCE, 1583-1595.
- Finno, R.J., Cosmao, T. and Gitskin, B. (1989). Results of foundation engineering congress pile loading test. *Symposium on Predicted and Observed Behavior of Piles, GSP 23*, R. J. Finno, Ed., pp. 338-355.
- Finno, R.J., Achille, J., Chen, H.C., Cosmao, T., Park, J.B., Picard, J.N., Smith, D.L. and Williams, G.P. (1989). Summary of pile capacity predictions and comparison with observed behavior. *Symposium on Predicted and Observed Behavior of Piles, GSP 23*, R.J. Finno, Ed., ASCE, pp. 356-382.
- Goudreault, P.A. and Fellenius, B.H. (1999). *UniPile Version 4.0 for Windows. Users Manual*, UniSoft Ltd., Ottawa, [www.UnisoftLtd.com] 64 p.
- Kathol, C.P. and McPherson, R.A. (1975). Urban geology of Edmonton, Alberta. *Research Council Bulletin 32*, Alberta Research Council, 92 p.
- Likins, G.E., Fellenius, B.H. and Holtz, R.D. (2012). Pile Driving Formulas—Past and Present. ASCE Geo-Institute Geo-Congress Oakland, March 25-29, 2012, *Full-scale Testing in Foundation Design, State of the Art and Practice in Geotechnical Engineering, GSP 227*, ASCE, Reston, VA, M.H. Hussein, K.R. Massarsch, G.E. Likins, and R.D. Holtz, eds., pp. 737-753.